Four-dimensional (4D) image reconstruction strategies in dynamic PET: Beyond conventional independent frame reconstruction

Arman Rahmim[a] and Jing Tang
Department of Radiology, Johns Hopkins Medical Institutions, Baltimore, Maryland 21287

Habib Zaidi
Division of Nuclear Medicine, Geneva University Hospital, CH-1211 Geneva 4, Switzerland

(Received 29 December 2008; revised 5 June 2009; accepted for publication 8 June 2009; published 10 July 2009)

In this article, the authors review novel techniques in the emerging field of spatiotemporal four-dimensional (4D) positron emission tomography (PET) image reconstruction. The conventional approach to dynamic PET imaging, involving independent reconstruction of individual PET frames, can suffer from limited temporal resolution, high noise (especially when higher frame sampling is introduced to better capture fast dynamics), as well as complex reconstructed image noise distributions that can be very difficult and time consuming to model in kinetic parameter estimation tasks. Various approaches that seek to address some or all of these limitations are described, including techniques that utilize (a) iterative temporal smoothing, (b) advanced temporal basis functions, (c) principal components transformation of the dynamic data, (d) wavelet-based techniques, as well as (e) direct kinetic parameter estimation methods. Future opportunities and challenges with regards to the adoption of 4D and higher dimensional image reconstruction techniques are also outlined.
[DOI: 10.1118/1.3160108]

Key words: PET, spatiotemporal, dynamic imaging, four-dimensional (4D), five-dimensional (5D)

I. INTRODUCTION

Modern molecular imaging techniques are expected and being seen to result in a revolutionary paradigm shift in healthcare and clinical practice. Among the unique features of positron emission tomography (PET) is that it is a quantitative imaging modality by nature.[1] Another important aspect of PET is its inherent ability to perform dynamic imaging taking advantage of the high sensitivity achieved by stationary multiring systems.[2,3] This is a very notable capability allowing measurements of change in the biodistribution of radiopharmaceuticals within the organ(s) of interest over time. This, in turn, offers very useful information about the underlying physiological or metabolic processes, as commonly extracted using various kinetic modeling techniques.[4] By comparison, SPECT imaging typically requires camera rotations to achieve complete angle tomography, thus limiting how fast each frame may be acquired. It is worth noting though that alternative approaches to dynamic SPECT have been proposed, allowing slow camera rotations (e.g., even a single rotation for the entire study); i.e., yet they typically require making certain assumptions about the functional behavior of the tracer.[3] In the context of dynamic PET imaging (similarly applicable to stationary SPECT or conventional SPECT in which complete tomographic data are available for each frame), we next outline the three standard steps commonly performed.

I.A. Dynamic PET acquisition, reconstruction, and kinetic parameter estimation

Dynamic PET acquisition can be performed using two general approaches depending on whether the scanner has the list-mode acquisition capability; i.e., the ability to store time of detection along with the spatial coordinates (and energy) for the detected events.[5] If such ability does not exist, the standard approach is to prespecify, prior to data acquisition, the framing sequence of interest and to bin the detected events in the corresponding sinograms to each frame. By contrast, the list-mode acquisition capability allows the added flexibility of specifying the framing sequence postacquisition.

Following dynamic framing of the acquired data as outlined above, the common approach to dynamic PET image reconstruction consists of independently reconstructing tomographic data within each dynamic frame. Following this step, one arrives at a set of dynamic images intended to specify the variation in activity over time throughout the reconstructed field of view. This is still the *de facto* standard approach applied in routine clinical studies in many institutions.

Following the reconstruction step, the underlying functional parameters of interest [e.g., binding potential, maximum binding potential B_{max}, dissociation constant of binding K_d, etc.] can be obtained using a number of tracer kinetic modeling techniques.[4] Most commonly, compartmental modeling techniques are utilized and are applied to time activity curves (TACs) extracted for either (i) particular regions of interest (ROIs) or (ii) at the voxel level, the latter resulting in parametric images.

I.B. Issues with conventional dynamic imaging

The aforementioned standard approach to dynamic PET imaging suffers from three main issues:

(i) The independent reconstruction of each of the (typically) many frames of the data can result in very noisy images.
(ii) Conventional dynamic PET reconstruction incorporates only the data from within each frame (and not any other) to arrive at the image for that frame, imposing a limitation on the temporal resolution of the scanner and its ability to capture the dynamics. While increasingly higher temporal framing may be utilized, this will, in turn, result in even higher noise levels (these two issues may thus be expressed in terms of a noise vs. temporal resolution trade-off).
(iii) Accurate application of tracer kinetic modeling requires knowledge and modeling of the noise distribution present in the reconstructed dynamic images (how noisy individual voxels are and how they correlate with other voxels), which can be extremely difficult and time consuming to perform.[6,7] As a result, very commonly, the presence of space-variant noise variance and intervoxel correlations are simply ignored in kinetic parameter estimation.

In this review, we refer to the field encompassing techniques that attempt to address one or more of the aforementioned three issues as spatiotemporal four-dimensional (4D) PET image reconstruction. A wide range of methods have been proposed in literature to this end,[8–10] and they all agree in that they do *not* independently reconstruct individual dynamic frames, and these methods aim to outperform conventional dynamic PET [e.g., in terms of precision (noise) vs accuracy (bias) trade-offs].

We have identified and elaborated upon five categories of strategies that can be classified as 4D PET image reconstruction: These are techniques that utilize (a) iterative temporal smoothing, (b) advanced temporal basis functions, (c) principal components transformation of the dynamic data, (d) wavelet-based techniques, and (e) direct kinetic parameter estimation methods. Each of these categories is presented in Secs. II–VI, respectively. For further clarity, a more concise summary of these techniques, along with their advantages, drawbacks/limitations, as well as outstanding issues to investigate, has been presented in Table I. A number of future opportunities and challenges in the field of multidimensional (4D and higher) image reconstruction have been outlined in Sec. VII, followed by concluding remarks in Sec. VIII. Before moving on to the review section, we wish to make the following two observations.

I.B.1. Relation with motion-compensation techniques

We wish to note that dynamic imaging and motion-compensated imaging methods overlap in the sense that they both deal with varying activity distributions over time. Yet one must note that the underlying bases of the two are different and need to be distinguished from one another; for the latter, for instance, some types of motion (and thus certain changes in voxel intensity) are physically/anatomically impossible. As such, this review focuses on dynamic imaging, while techniques to model and incorporate motion have been reviewed elsewhere (e.g., Rahmim *et al.*[52]). On a related note, we believe that techniques, which attempt to apply general 4D PET image reconstruction methods to motion compensation (e.g., Grotus *et al.*[53] and Verhaeghe *et al.*[54]), remain to be further validated to ensure that the estimated motion vector fields are physically allowed.

I.B.2. List-mode vs histogram-mode 4D PET image reconstruction

It is worth emphasizing that list-mode acquisition is distinct from list-mode reconstruction; the former (increasingly employed in current PET scanners) is only a prerequisite for the latter. The initial and primary motivation behind list-mode image reconstruction was to provide a fast and accurate technique given the fact that increasingly less counts per histogram bin are being produced by PET scanners: This can be due to increasing lines of response for modern PET scanners, time-of-flight PET, or dynamic PET with increasingly short frames, any or a combination of which can result in counts per histogram bin to approach the order of unity and even (much) less.[2,55–60] As a result, it may be more efficient to process individual events, as opposed to histogram bins. Furthermore, in the context of motion compensation, direct list-mode image reconstruction can be more feasible and advantageous.[61]

In dynamic PET, list-mode reconstruction may introduce an additional benefit. As 4D image reconstruction techniques move beyond independent frame reconstruction of data, having access to time of acquisition information for events can be valuable. The basic idea, put simply, is that an event detected toward the end of a particular frame has more information to convey about subsequent frames than an event detected earlier, whereas this information is not available in histogram-mode acquisition (see Sec. III B).

II. ITERATIVE TEMPORAL SMOOTHING

II.A. A common approach

A common approach in this direction has been to impose temporal voxel smoothing within the reconstruction task. This has been implemented via:

(i) Interiteration temporal smoothing[11] in which high-frequency noise filtering is performed after every iteration of the reconstruction algorithm, with the assumption of similarity between nearby frames.
(ii) Maximum *a posteriori* probability (MAP) image reconstruction: In the standard framework, MAP-based methods seek to minimize variations between spatial neighboring voxels. This is also referred to as the Bayesian method (originally derived from a simple application of Bayes' rule to image reconstruction). It is also, sometimes, referred to as penalized likelihood

TABLE I. Outlined strategies for spatiotemporal 4D PET image reconstruction. Representative references directly discussing each strategy are also mentioned. Other references related to aspects of the strategies are mentioned in the text.

Category	Technique	Specific approach	Key advantages	Drawbacks/limitations	Issues to investigate
Iterative temporal smoothing (Sec. II)	Common approach (A) (Refs. 11 and 12)	Imposing smoothing between temporally neighboring voxels within the reconstruction task	Some improvements in noise performance	*Ad hoc* assumption that temporally neighboring voxels have similar intensities	Conditions for convergence
	Model-based temporal smoothing (B) (Refs. 13 and 14)	Fitting of intermediately generated TACs by a kinetic model as a noise reduction technique.	Noise reduction of iterative images is based on models reflecting underlying dynamic mechanism.	Application of kinetic model to images that have not converged yet may result in overall divergence	How early in the iterative task can this model-based smoothing be safely imposed? How strongly?
Use of advanced temporal basis functions (Sec. III)	Model-based basis functions (A) Ref. 15	Temporal sampling of the data using task-based, model-driven, theoretical curves	Temporal basis functions utilized are physiologically relevant and meaningful.	Requiring in advance knowledge and modeling of the particular task of interest	Optimization techniques for the selection of number and distribution of basis functions
	Interpolating basis function (B) (Refs. 16–18)	Temporal sampling of the data using compact and efficient (e.g., B-spline) basis functions	Can be utilized if no prior knowledge of kinetic model is available	Shapes of temporal basis functions not adapted to the particular task or data of interest	Does nonuniform temporal sampling notably improve image reconstruction? Robust optimization of nonuniform sampling schemes
	Data-driven temporal basis functions (C) (Refs. 19–21)	Temporal basis functions are generated for each particular study, either based on analytic decomposition of initially reconstructed dynamic images, or estimated jointly with the images	The basis functions are tailored specifically to each data set and are not determined *a priori*. They can even be adaptively redefined (C-2).	Basis functions may contain negative values (SVD method). Stability and convergence issues (inter-reconstruction method)	In practice, do these basis functions outperform other nondata-driven basis functions?
Principal component transformation of dynamic data (Sec. IV) (Refs. 22 and 23)		Transformation of dynamic PET data sets into the principal components domain, followed by independent reconstructions	Decorrelation of transformed dynamic data sets, thus allowing fast yet accurate reconstructions. Natural noise reduction by discarding high-order principal components (reduction in dimensionality).	Only shown to be applicable under the Gaussian likelihood function for the measured data	Number of principal components to utilize may be highly task-based: Need for optimization.

image reconstruction. This approach can be extended to a 4D MAP algorithm (e.g., see Ref. 12) in which one uses a summation of spatial and temporal potential functions in order to encourage smoothing between neighboring voxels in both the spatial and temporal domains.

TABLE I. (*Continued.*)

Category	Technique	Specific approach	Key advantages	Drawbacks/limitations	Issues to investigate
Wavelet-based techniques (Sec. V)	Postprocessing techniques (A) (Refs. 24–30)	Application of temporal denoising of dynamic images, or alternatively, performance of kinetic modeling in the wavelet transform domain	Computationally less demanding, while making use of the inherent ability of wavelets to localize information in the time-frequency domain for noise reduction	As this method is applied post-reconstruction, it does not have the flexibility of performing additional regularization as used in the next technique	How do post-reconstruction methods compare with reconstruction-based wavelet techniques?
	Reconstruction-based techniques (B) Ref. 31	Use of wavelets as temporal basis functions: exponential-spline (E-spline) wavelets assuming activity ruled by a system of differential equations involving compartmental models	Allowing application of regularization techniques within the wavelet-based reconstruction methods, thus to control noise	Complicated parameter selection for the proposed E-spline wavelets (based on differential models that need to be known *a priori*)	Do wavelets outperform other basis functions as mentioned in Sec. III?
Direct kinetic parameter estimation (Sec. VI)	Generation and reconstruction of parametric sinograms (A) (Refs. 32–38)	Performing kinetic modeling and fitting in the projection-domain, followed by a single reconstruction	Improved speed performance	Applicable only to linearized kinetic models	Need for reconstruction algorithms that model nonPoisson nature of parametric sinograms
	Direct estimation from noncombined dynamic data (B) (Refs. 5 and 39–51)	Direct estimation of the parametric image itself, by relating it to the measured data	Straightforward data-space noise modeling for parameter estimation, as it removes the need to model complex reconstructed image noise distributions. Convergent EM algorithms for linear models.	Kinetic model has to be applicable throughout the image. A nonlinear estimation problem for nonlinear kinetic models, which can be computationally expensive.	Conditions for convergence of nonlinear kinetic models. Stability issues for nonlinear kinetic models with increasingly unknown kinetic parameters to be estimated.

Application of these approaches to dynamic PET (or SPECT) imaging has been shown to improve the noise performance of the reconstruction algorithms; nevertheless, they are *ad hoc* in the sense that they assume *a priori* that voxels in neighboring temporal frames have close values, and as such are bound to perform poorly for frames with fast dynamics. It must be noted that the application of such methods in the context of motion compensation, as reviewed in Ref. 52, is better conditioned since one can incorporate the extracted motion information within the 4D smoothing task[62–64] and not simply assume that each voxel has nearly constant values in nearby frames. In the rest of this paper, we describe techniques that attempt to more accurately model the underlying dynamic mechanism within the 4D image reconstruction task.

II.B. Model-based temporal smoothing

Instead of encouraging temporally adjacent voxels to have similar values, it makes more sense to encourage them to have intensity values along a kinetic fitted curve, as first investigated by Kadrmas and Gullberg[13] within the MAP framework. Thus, this approach effectively performs temporal smoothing of the intermediate images based on a parametric kinetic model. The extreme special case of this method, investigated by Reader *et al.*,[14] would simply replace the intermediate image estimates by the corresponding intensities found by fitting at each iteration. An example result from this kind of algorithm is shown in Fig. 1. In general, while this overall approach appears more promising that the previous one (Sec. II A), it is not known to be convergent and, in fact, suffers from the potential problem that a specific

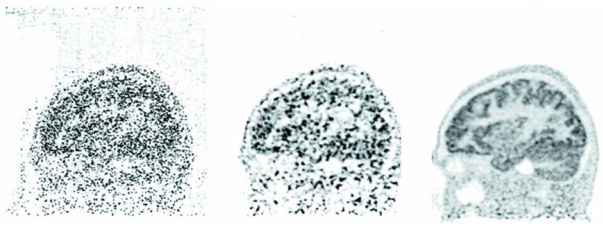

FIG. 1. Impact of 4D PET reconstruction for one 5 min frame of a 60 min [^{11}C]-flumazenil study acquired on the brain dedicated high resolution research tomograph. Shown is a sagittal slice reconstructed using an EM algorithm based only on the line-integral model (left); the same slice reconstructed with list-mode EM including a resolution model with the line-integral model (middle); and the same slice reconstructed using a 4D method (right)—which is able to benefit from all 60 min of data without compromising temporal resolution (although this is, of course, dependent on the type of temporal basis functions chosen or estimated). Reprinted with permission from Ref. 9.

kinetic model applied to intermediate image intensities that have not yet converged does not necessarily perform well, and thus does not necessarily result in improved algorithmic performance. It remains to investigate how early in the iterative reconstruction, and how strongly, this model-based temporal smoothing can be applied while warranting real or effective convergence in the overall algorithm.

III. USE OF SMOOTH TEMPORAL BASIS FUNCTIONS

As mentioned in Sec. I A above, conventional dynamic PET imaging methods specify framing sequences within which the data are independently reconstructed. This can be thought of as using the simplest possible temporal basis function, namely, the rectangular pulse, in the reconstruction task such that the data acquired in a particular frame do not contribute at all to other temporal frames. That is, reconstruction of independent time frames ignores temporal correlations.

An alternative approach would then aim at using other smooth temporal basis functions in order to improve the quality of images by better relating the data measured in different (especially adjacent) frames. The use of temporally extensive basis functions allows each time point in the time-series reconstruction to draw from more, if not all, of the acquired data.[9] Let us consider N temporal basis functions where $B_k(t)$ is used to denote the kth basis function ($k=1,\ldots,N$). Then, the dynamic image set can be represented as

$$\lambda_j(t) = \sum_{k=1}^{N} w_{jk} B_k(t), \tag{1}$$

where $\lambda_j(t)$ represents the image intensity at location j at time t, and w_{jk} is the coefficient of the kth basis function at location j. In this context, the reconstruction task becomes to estimate the coefficients of the basis functions.

Various related approaches have been studied in literature, which we classify below in terms of how the basis functions are defined: Namely, whether they are (i) model based, (ii) interpolating, or (iii) data driven, as we discuss next.

III.A. Model-based basis functions

It makes sense to consider basis functions extended temporally in accordance with some physiologically meaningful dynamic models describing how activity distribution varies over time. Meikle *et al.*[15] used the approach of spectral analysis in which the basis functions were modeled as exponential functions of varying widths convolved with the arterial input function $q(t)$, as initially proposed in Ref. 5,

$$B_k(t) = q(t) \otimes \exp(-\beta_k t). \tag{2}$$

In this technique, the β values were fixed and chosen to cover the spectrum of the expected kinetic behavior (for the particular biological imaging task). The authors then used the expectation-maximization (EM) technique to estimate the w coefficients [Eq. (1)] of the basis functions from the data. This overall approach is somewhat specific to the imaging task of interest (range of β values need to be determined in advance); however, it can be applied to a wide range of radiotracers since spectral analysis has the advantage of not preselecting a particular compartment model for the radiotracer kinetics.[65]

In the context of planar gamma camera imaging (no reconstruction involved), Nijran and Barber[66] proposed to generate a large range of model-based theoretical curves from a particular tracer kinetic model and then use principal component analysis (PCA) as applied to the covariance matrix between the generated curves to generate the most significant principal components, best representative of the data. This is because PCA is designed to generate vectors with maximized variations between them, such that only a small number of these principal components suffice for an adequate description of time variations at any voxel (also achieving noise reduction). A relevant extension of this approach to 4D PET, not explored in literature to our knowledge, would be to use such generated principal components as temporal basis functions in the reconstruction tasks as applied to dynamic PET data. The aforementioned model-based techniques have the advantage of utilizing physiologically indicative basis functions. At the same time, they are limited in that they require in advance knowledge on the range of modeling parameters to be used in the generation of the basis function. Section IV discusses an alternative 4D approach also making use of the principle component technique, but this time to transform the dynamic data itself prior to reconstruction.

III.B. Interpolating basis functions

In cases where the particular kinetic model is not known in advance, or is not accurately characterized, it is more desirable to consider temporal basis functions that are model independent. Interpolating basis functions fit this criterion. The original motivation for their increasing use in the reconstruction tasks[16–18,67] can be seen by the following simple observation: The assumption that activity is constant within each dynamic frame, as used in conventional reconstruction

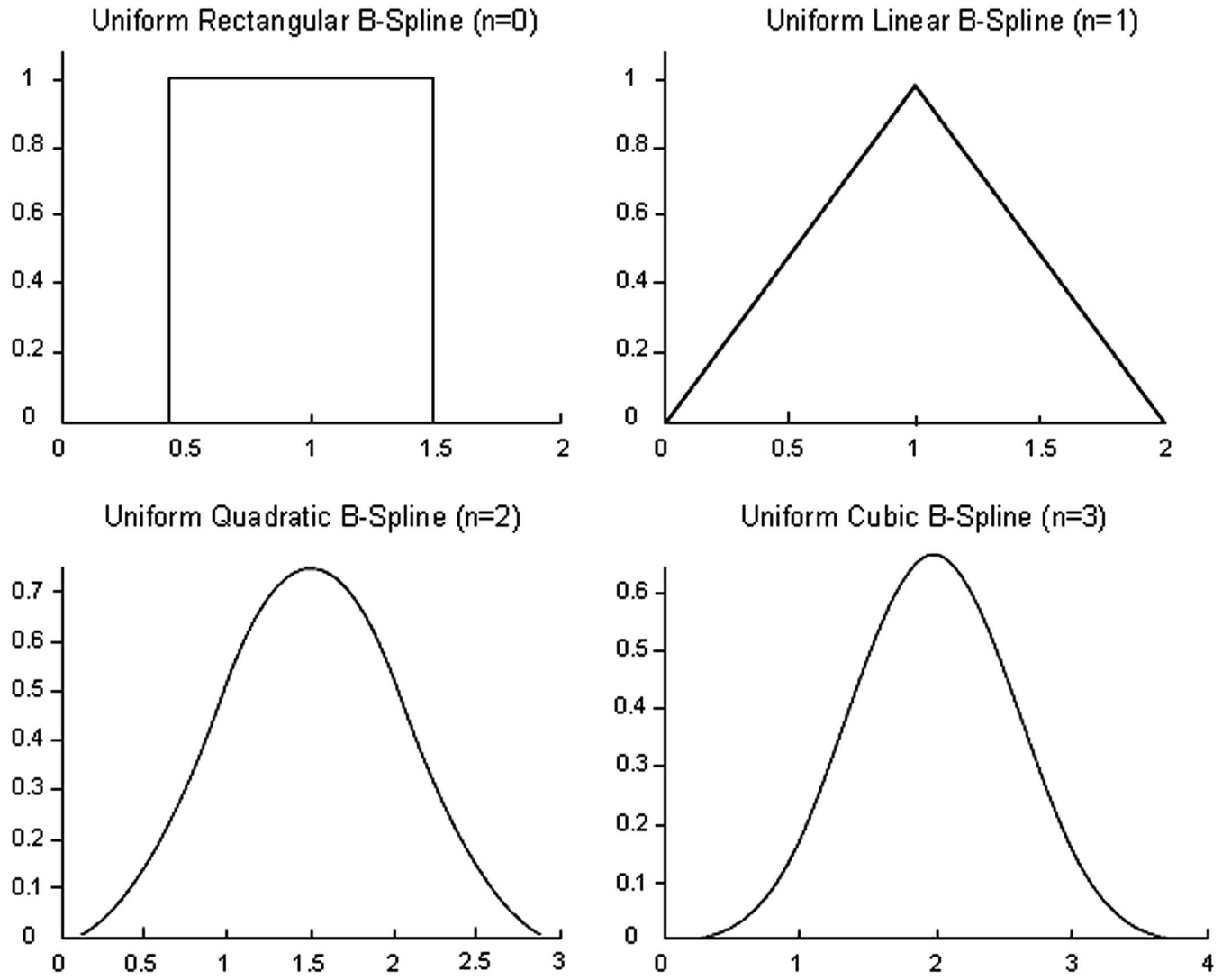

FIG. 2. B-spline basis functions of increasing orders ($n=0-3$).

techniques (see Sec. I A), is essentially equivalent to performing nearest-neighbor interpolation when considering a detected event; i.e., using a very simple rectangular pulse temporal basis function so that each event only contributes to the dynamic frame in which it is detected.

Alternatively, one may consider utilizing interpolating basis functions to better sample the temporal variation in activity in each voxel. In fact, such an approach is commonly employed in the spatial domain: (i) In image representation, where relatively smooth basis functions are used to more accurately represent spatial activity distribution compared to using voxels (e.g., spherically symmetric "blob" basis functions[68,69] or "natural pixels"[70–72] were considered), and (ii) in forward-/back-projection operations where more advanced interpolation techniques are utilized to improve images obtained compared to merely using nearest-neighbor interpolations.

A similar logic applies to the temporal domain where it makes very good sense to consider more sophisticated temporal basis functions so as to move beyond the commonly used nearest-neighbor temporal interpolation scheme. In this regard, of very considerable potential and use have been the B-spline basis functions.[73–75] These functions are very easily obtained by convolutions of the rectangular pulse function, as depicted in Fig. 2. Thus the zeroth-order B-spline function is the rectangular function itself, corresponding to the nearest-neighbor interpolation, while the first-order function is the triangular function that is used for linear interpolation, and increasing orders correspond to higher degrees of interpolation.

B-spline basis functions have been shown to have very favorable properties including being compact (thus efficient to implement) while minimizing errors (i.e., they fast approach the ideal interpolating function with few increasing orders). In fact, nowadays it is the third-order cubic B-spline function that is most commonly used to sample the spatial or temporal domain as it has very favorable efficiency/accuracy properties. This is in contrast to the ideal sinc function interpolator, which is exact but does not have finite support and thus cannot be sampled efficiently.

In this context, a number of different reconstruction algorithms that aim to estimate the w coefficients in Eq. (1) have been proposed by a number of researchers and directly applied to list-mode[16,17] or histogrammed data.[18] They have been shown to result in kinetic parameter estimates with improved precision vs accuracy trade-offs compared to conventional dynamic PET image reconstruction. Furthermore, these reconstruction algorithms were designed and shown to be convergent.

It is worth noting that (as also mentioned in Sec. I B 2) application of list-mode 4D image reconstruction is expected to be in advantage over the histogram-mode counterpart. This is because it can be presumed that compared to events measured at the beginning of a frame m, the data measured toward the end of that particular frame contain more information about the basis function coefficient for the next frame $(m+1)$, and that by performing histogramming, this additional information is lost. By contrast, direct list-mode reconstruction maintains this information in the reconstruction task. Nonetheless, conclusive databased evidence of the list-mode 4D reconstruction technique outperforming the histogram-mode method remains to be demonstrated.

It must be noted that in the aforementioned works, the authors considered the use of nonuniform basis functions since early changes in concentration are typically much greater than those observed later in the study, and thus it makes sense to sample the temporal domain nonuniformly. This problem may also be thought of as finding the basis functions whose span covers the true TACs (a general problem for TAC estimation, regardless of the issue of image reconstruction), while suggesting the use of adaptive basis function sampling techniques.[18] Robust optimization of such nonuniform sampling remains to be fully studied, especially using analytic methods.

III.C. Data-driven temporal basis functions

In the aforementioned general approach, the shapes of the temporal basis functions are determined *a priori* independent of the particular study (though the nonuniform sampling scheme, if performed at all, is often dependent on the study). An alternative is to instead use methods that determine the shapes of the basis functions in a data-driven sense. Below we describe two such approaches used in literature for the task addressed in this paper.

III.C.1. Basis functions derived by analytic decomposition of dynamic images

Matthews *et al.*[19] used singular value decomposition (SVD), as applied to dynamic PET images initially obtained using conventional reconstruction, in order to arrive at a set of useful temporal basis functions to be used in subsequent 4D image reconstruction [the EM formalism was used in this work to estimate the w coefficients in Eq. (1)]. The SVD technique has the advantage that in practice many of the singular values are insignificant when compared to the other dominant singular values, thus requiring only a subset to be used in the estimation task. Overall, this technique does not assume a kinetic model at all and based its results on a set of dynamic images initially obtained via standard reconstruction. A complication with this technique is that the resulting basis functions may contain negative values.

It is natural to impose positivity constraints in PET imaging given the known problems of negative artifacts in PET. Iterative reconstruction methods often use a positivity constraint and thus are automatically tuned to be non-negative. Given the count-limited nature of the acquired data in dynamic imaging, there are advantages in considering basis functions which are nonorthogonal and which overlap in spacetime.[9] It should be noted that the positivity constraint in static PET imaging is a much more difficult constraint in dynamic PET imaging characterized by the acquisition of low count studies. This is particularly true when basis functions that have negative values are used, excluding the case of nonoverlapping rectangular basis functions. The mixture models proposed by O'Sullivan[76] stand for time course data at the voxel level presented in the form of a convex linear combination of a number of principal time activity curves, referred to as sub-TACs, each characterized by its individual spatial distribution. The main difficulty is that positivity constraints on the sub-TACs are not enough to guarantee a sensible physiological interpretation of the sub-TACs.[77] Other approaches to circumvent this limitation, including postprocessing iterative techniques that allow to adjust negative values by cancellation with positive values in a surrounding local neighborhood, have been developed.[78]

Alternatively, a data-driven PCA approach (unlike model-based approach as discussed in Sec. III A) could also be utilized; i.e., PCA basis functions may be extracted from a preliminary reconstruction of the dynamic data and utilized in a new 4D image reconstruction. The performance of such a PCA approach could be improved by performing kinetic prenormalization to create clearer margins and improved contrast between different regions in the resulting images by reducing the pixel values for regions having the same kinetic behavior as shown in dynamic brain PET images.[79] An example is shown in Fig. 3 which illustrates the first principal component (PC1) image using [^{11}C]-5-hydroxy-*L*-tryptophan (HTP) in a healthy volunteer, compared to images obtained using reconstructions of a static image of a predefined frame, sum images for various combinations of dynamic frames and parametric images obtained using Patlak linear model. The results show an improved image quality and better discrimination between areas with different levels of tracer utilization while retaining a low noise level compared to images generated using other techniques.[80,81]

III.C.2. Adaptive, inter-reconstruction estimation of basis functions

An alternative approach has been to perform 4D reconstruction whereby the temporal basis functions themselves are also estimated as part of the reconstruction process,[20] thus allowing the adaptive redefinitions of the basis functions throughout the reconstruction task.

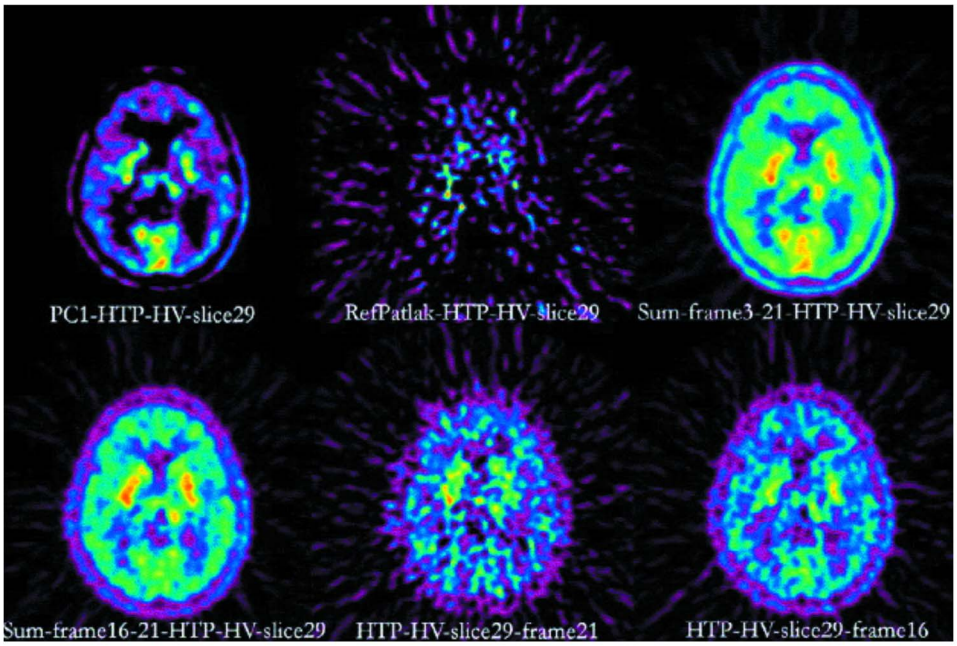

FIG. 3. Representative slice of a dynamic human brain PET study using HTP in a human volunteer showing results obtained using PCA and other reconstruction modes. The PC1 is compared to reference Patlak linear model applied on input data from 20 to 60 min, sum images (frames 3–21), sum images (frames 16–21), image from frame 21 only, and finally same image from frame 16. Reprinted with permission from Ref. 80.

This was implemented using an approach in which one first fixes the temporal basis functions (treating them as known), estimates the corresponding w coefficients [see Eq. (1)], and then alternates to an estimation algorithm in which the w coefficients are held as fixed and known, while the distributions of the temporal basis functions (at various temporal sampling points) are determined. It must be noted that here when temporal basis functions are being estimated (jointly with basis function coefficients), there still needs to be a model for those basis functions—typically as linear combinations of simpler basis functions such as nonoverlapping rectangular functions.

A simultaneous updating procedure, not requiring to prespecify the number of iterations inside each of the above two steps before switching to the other, was also outlined in Ref. 21 nearly halving the computation time. However, this approach is not convergent and may have some stability issues.

Overall, this technique, though potentially very promising, is not convergent globally. Furthermore it remains to be studied whether the proposed data-driven determination of the basis functions outperforms the previous reconstruction algorithms outlined in Sec. III B.

IV. PRINCIPAL COMPONENT TRANSFORMATION OF THE DYNAMIC DATA

An alternative approach consists of performing principal component transformation, or analysis (PCA), on the dynamic data along the temporal direction. This is also sometimes referred to as the Karhunen–Loève (KL) transform. The term KL, however, is best applied to cases when the true ensemble covariance (and not the estimated sample covariance as is done in PCA) is known. Thus, in the experimental task of PET imaging where the object distribution is not known *a priori*, it makes sense to use the term PCA. PCA is a popular technique for many years in various fields, particularly in geosciences and remote sensing, used to decorrelate multispectral images as used in compression, denoising, and deblurring. It is also one of the most commonly used multivariate analysis tools in brain PET imaging[80–84] and has been used by a few investigators for the analysis of oncological PET data.[85]

In the context of dynamic imaging, the general idea is that application of PCA to a time series of images allows their decomposition into a number of factor images which are uncorrelated (i.e., with maximized variations between them). Since in practice only few of the factor images are sufficient to adequately describe the underlying dynamics, removal of the negligible factors renders a natural noise reduction technique. Such a denoising approach has been applied in the past to conventional dynamic nuclear medicine imaging (e.g., model-based approach described in Ref. 66, as reviewed in Sec. III.A.1, and model-independent dynamic sinogram noise reduction work of Kao *et al.*[86]). It must be noted that in the context of TAC extraction and noise reduction, factor analysis techniques other than PCA have also been explored; e.g., see the works by El Fakhri *et al.*[87] and Su *et al.*[88] for brief reviews and some novel techniques.

In the context of 4D image reconstruction, Wernick *et al.*[22] made the observation that dynamic image sets in their standard forms are correlated in the temporal direction and thus require 4D reconstruction algorithms that model and incorporate such temporal correlations (various approaches to this were discussed in previous sections). By contrast, the

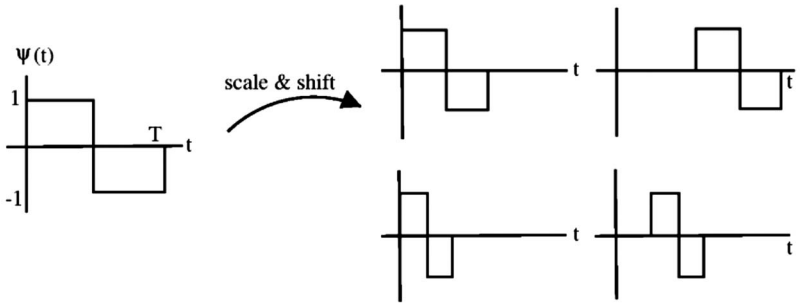

FIG. 4. Haar wavelet: Mother wavelet and some daughter wavelets.

authors proposed to first transform the standard dynamic datasets using PCA and showed that, with some simplifying assumptions, the resulting dynamic datasets become nearly uncorrelated and thus can be reconstructed independently, resulting in fast yet accurate reconstructions. Furthermore, computational gains could be made by discarding high-order principal components to avoid reconstructing them.

The aforementioned derivations were only made for a weighted least-squares likelihood function (thus a Gaussian likelihood model for the measured data) and not for the Poisson statistic of noncorrected PET data. Furthermore, while a general advantage of the PCA approach is that the dimensionality of any dataset can be potentially reduced, the selection of the number of principle components to utilize can be very case specific and will have to be determined and optimized for each particular task of interest.

We conclude this section by noting that even though the aforementioned approach is originally designed for imaging of motion-free objects, it has been shown to work very well in reconstructing cardiac image sequences as well,[23] and this is hypothesized[22] to be the case because the principal component model is able to capture the motion information in the form of motion-induced temporal fluctuations of the signal.

V. WAVELET-BASED TECHNIQUES

Wavelets are powerful mathematical tools for analysis of finite, nonperiodic, and/or nonstationary signals. Wavelet transforms (WTs) differ from traditional Fourier transforms by their inherent ability of localizing information in the time-frequency domain. The wavelets are scaled and translated copies (known as "daughter wavelets") of a finite-length or fast-decaying oscillating waveform (known as the "mother wavelet"). As an example, the first known and also the simplest possible wavelet is the Haar wavelet with its mother wavelet function $\psi(t)$ described as

$$\psi(t) = \begin{cases} 1, & 0 \le t < 1/2 \\ -1, & 1/2 \le t < 1 \\ 0, & \text{otherwise}. \end{cases} \quad (3)$$

Figure 4 shows the mother wavelet of Haar wavelet with some of its daughter wavelets.

Wavelets and multiscale methods have been widely applied in PET imaging. They have been applied in PET image analysis tasks such as segmenting image structures in clinical oncology.[89] In quantitative analysis, multiscale denoising has been applied to postprocess dynamic PET images at the voxel or ROI level. Before their specific application in emission tomographic reconstruction, wavelets were incorporated in solving linear inverse problems, for example, with wavelet-vaguelette[90] and vaguelette-wavelet[91] decompositions, followed by thresholding. Kolaczyk[92] applied the aforementioned wavelet-vaguelette decomposition as well as wavelet shrinkage (WS) (Ref. 93) in tomographic image reconstruction of individual frames in the context of the analytic FBP algorithm. Multiscale analysis and regularization was also applied in statistical restoration and reconstruction (also single frame).[94–97] WS was used as an interiteration filter in the OSEM reconstruction process to achieve simultaneous edge preservation and noise reduction.[98] As we review next, wavelets have also been applied to spatiotemporal reconstruction of dynamic PET images.

V.A. Wavelet postprocessing in dynamic PET

In the context of dynamic imaging, the one-dimensional wavelet transform has been applied in designing a time-varying filter to improve the signal-to-noise ratio (SNR) in PET kinetic curves.[24] A two-dimensional wavelet denoising algorithm was applied by Lin and co-workers[25,26] to each short-axis image plane (of each individual image) independently in order to remove noise in the spatial domain, followed by application of one-dimensional wavelet denoising to the TAC for each ROI so as to also remove noise in the temporal domain.

Turkheimer and co-workers[27,28] and Cselényi *et al.*,[29] followed by Arhjoul and Bentourkia,[30] performed kinetic modeling in the wavelet domain. They applied the dyadic wavelet transform (e.g., using James–Stein or Battle–Lemarie filters) to each dynamic frame to produce the correspondent wavelet transform. Kinetic modeling was then applied to wavelet coefficients of the dynamic frames. The motivating idea behind this approach is that wavelet coefficients are (i) sparse, i.e., information is compressed in fewer coefficients of greater magnitude (resulting in effective thresholding to achieve shrinkage and noise reduction, prior to performing the inverse wavelet transform), and (ii) whitening or decorrelation effect between the wavelet coefficient, suggesting more feasible kinetic modeling in the wavelet domain. Arhjoul and

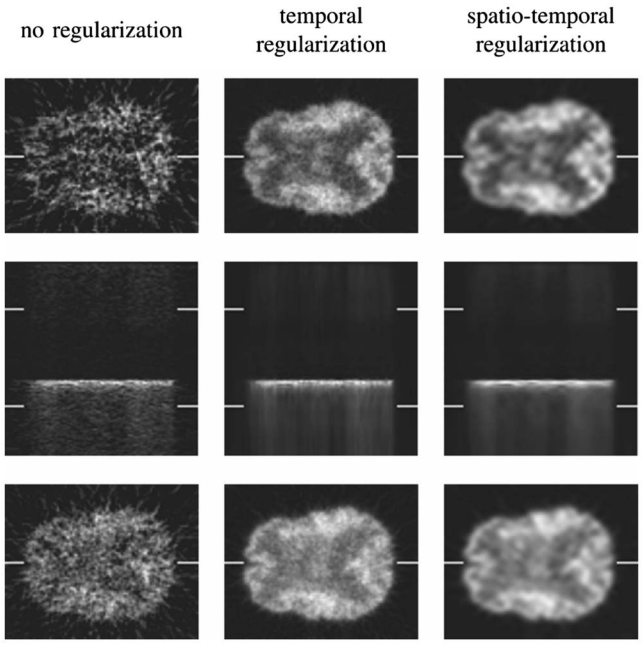

FIG. 5. Reconstructed brain phantom slices. Middle row are temporal slices. Time and space locations are indicated by the white bars. Upper and lower spatial slices correspond with the upper (early time) and lower (late time) bars in the temporal slice, respectively. Results in the third column give a good compromise between spatial and temporal regularization. Reprinted with permission from Ref. 31.

Bentourkia used a similar approach to perform kinetic modeling in the projection space[32] (method of "parametric sinograms"), which is reviewed in Sec. VI A.

V.B. Wavelet-based reconstruction

Although noticeable research has been performed in using tailored temporal basis functions for representing the time activity curves in dynamic PET reconstruction (see Sec. III), Verhaeghe *et al.*[31] pioneered the research in using temporal wavelet basis functions. The L1-norm of the spatiotemporal wavelet coefficients of images served as the regularization term in the cost function to be minimized. Wavelets that were separable in space and time were utilized, with so-called B-spline wavelets in the spatial domain and E-spline wavelets in the temporal domain. The introduction of exponential-spline (E-spline) wavelets in the temporal domain was based on the concept that the activity distribution in the body is ruled by a system of differential equations involving compartmental models.

In a couple of dynamic PET simulations, one with a slice of the NCAT cardiac model and the second with a slice of the Zubal brain model, the regional SNRs from reconstructed noisy images were shown to be higher when temporal E-spline wavelets were applied compared to the case when temporal B-spline wavelets are used. The TACs extracted from a pixel in the left ventricle with wavelet regularization were shown to be closer to the true TAC. The spatiotemporal regularization reconstructed images were also shown to be less noisy than those with no regularization or with temporal regularization only (Fig. 5).

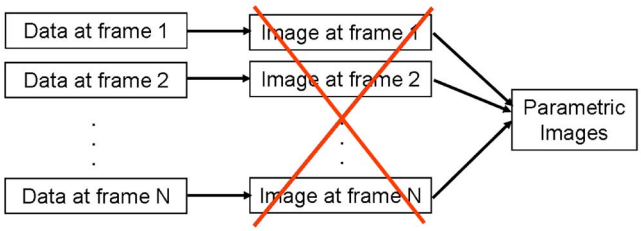

FIG. 6. Direct kinetic parameter estimation does not perform reconstruction of the individual frames and instead estimates the parametric image collectively and directly from the data.

We end this section by noting that the difference between the postprocessing and reconstruction-based techniques, wherein wavelet transform and shrinkage for localized denoising of time activity is applied following or during the reconstruction task, poses a familiar duality in imaging. It remains to be investigated whether the reconstruction-based approach is able to outperform its counterpart. Parallels for such needed comparison already exist in literature. For instance, in terms of noise reduction for static PET imaging, comparisons of postsmoothed maximum-likelihood (ML) reconstructed images with those obtained by MAP reconstruction in which smoothing is imposed within the reconstruction task have shown that (when requiring uniform spatial resolution) the results are actually not inferior,[99,100] with a theoretical argument given in Stayman and Fessler.[100] On the other hand, for the case when anatomical knowledge is available, the postprocessing technique has been demonstrated by theory and simulations to be inferior, unless noise correlations between neighboring voxels are taken into account (e.g., by applying a prewhitening filter).[101] In a very different context of motion compensation, reconstruction-based methods have been theoretically analyzed and compared to postreconstruction techniques and shown to be better suited to produce images of higher quality (similar bias, improved noise).[102] As mentioned above, such dual comparisons are still needed for the wavelet approach to dynamic PET image reconstruction.

VI. DIRECT KINETIC PARAMETER ESTIMATION

An alternative approach to conventional dynamic PET imaging has been to directly estimate kinetic parameters from the measured data instead of generating reconstructed PET images from which the kinetic parameters are estimated, as depicted in Fig. 6. Broadly, there have been two general approaches in this context: The first one designed to improve speed and the second one to improve accuracy, as we describe next.

VI.A. Generation and reconstruction of parametric sinograms

The technique consists of creating a parametric sinogram from multiple dynamic sinograms by performing some mathematical manipulation (given a particular kinetic model) in the projection space instead of the usual image space; this is then followed by a *singl*e reconstruction into the parametric

image. This method has the benefit of not performing reconstructions for each individual sinogram, thus reducing the computational burden by roughly one order of magnitude and has been investigated for different parameter estimation tasks by a number of investigators.[33–37] A more sophisticated approach[32] has been to estimate the parametric sinogram by first transforming the dynamic sinograms into the wavelet domain, followed by noise reduction and kinetic modeling, and finally synthesize back to the projection domain. This approach is motivated by the favorable properties of wavelets transforms [namely, sparseness and decorrelation effects (Sec. V A)].

A limitation of the method of parametric sinograms is that the kinetic models need to be expressed linearly in terms of the image-space activity such that they can be forward projected onto the data space. Examples of this include the Patlak formulation for irreversible binding, as opposed to a Logan type formulation for reversible binding which is nonlinear.[103] The latter, however, has been linearly reformulated[104] and has been used to directly generate parametric sinograms.[38] An additional issue is that while EM-type reconstruction algorithms assume that the data are Poisson distributed, the data in the parametric sinograms are not necessarily so (e.g., when one extracts the Patlak slope from dynamic sinograms, the slope of a fit to Poisson-distributed data is not Poisson-distributed itself). Reconstruction algorithms modeling this issue remain to be formulated and investigated.

VI.B. Direct parametric estimation from noncombined dynamic data

With regard to the three limitations of conventional dynamic PET imaging outlined in Sec. I B, while many techniques discussed so far in this review attempt to address the first two by improving noise vs temporal resolution performance, none address the third issue; i.e., the reconstructed images still contain very complex noise distributions that need to be modeled for accurate tracer kinetic modeling. For the sake of simplicity, kinetic modeling is typically performed with the assumption of uniform and uncorrelated noise across the image, thus neglecting the complexity of the noise variance and intervoxel correlations. A number of techniques have been proposed in order to obtain estimated parameters with reduced variance, including the use of ROI-based methods (requiring to assume voxels within each region having the same mean), as well as simple spatial regularization (assuming that neighboring voxels exhibit similar kinetic parameters),[105] ridge regression (application of variable penalty based on the deviation of fitted points from the regression line),[106] the wavelet transform,[28] or Markov random fields.[39] At the same time, it is plausible that accurately modeling the actual noise distribution in the images within the kinetic parameter estimation task can produce substantial improvements. While methodology has been developed in literature to estimate the noise distribution in the reconstructed images, including for the now common statistical, iterative image reconstruction techniques,[6,7] such accurate noise modeling remains to be studied for parameter estimation tasks.

At the same time, a more natural solution to this complication is to perform estimations of kinetic parameters directly from the dynamic data, having the advantage that the measured data are well known to follow the simple independently distributed Poisson distribution. This approach was originally and independently developed by Snyder[5] and Carson and Lange[40] in the very context of the EM algorithm modeling the Poisson noise distribution of the data. It sought to estimate kinetic parameters by maximizing the Poisson log likelihood of obtaining the measured dynamic data. The former was designed for a multicompartment model in which each mode had an exponential rate, with the amplitude and rate of each mode estimated by the EM algorithm, applicable to both histogram-mode and list-mode data, and was tested by a single simulation of a two-compartment model. The latter was instead formulated for histogram-mode data only, but for a very general kinetic model. The technique was tested for a simple single-tissue H_2O (Ref. 56) compartmental model.

In recent years, this problem has been revisited and more thoroughly developed and implemented by a number of different groups, as we review next. Just as there are two general categories of kinetic modeling techniques, namely, ROI based and voxel based,[4] we divide the direct estimation techniques in literature into these two general categories. For a more thorough comparison of direct parameter estimation techniques, Ref. 10 may also be consulted.

VI.B.1. ROI-based techniques

A number of techniques have been proposed that aim to directly estimate the kinetic parameters at the ROI level from the PET (or SPECT) dynamic data. Vanzi *et al.*[41] investigated a method to extract renal kinetic parameters for a simple model with one uptake constant for each kidney. Huesman *et al.*[42] and Zeng *et al.*[43] developed methods to extract kinetic parameters in myocardial imaging using one-compartment and two-compartment methods, respectively. These two contributions were also designed to better address the existing problem in standard reconstructions for dynamic SPECT imaging, in which the rotation of the detectors, while the distribution of the radiopharmaceutical changes over time, results in inconsistent projections.

The aforementioned methods first extracted the boundary information for the ROIs from standard reconstructions, followed by the application of direct ROI parameter estimation from the data. Alternatively, Chiao *et al.*[44] developed techniques that jointly estimate, within a single reconstruction task applied to cardiac dynamic emission tomography, both the kinetic parameter estimates as well as the boundary information. An approach was also developed by the same authors[45] to use boundary side information (obtainable from high resolution MRI and CT images) within a similar direct reconstruction scheme. This has the limitation that it will

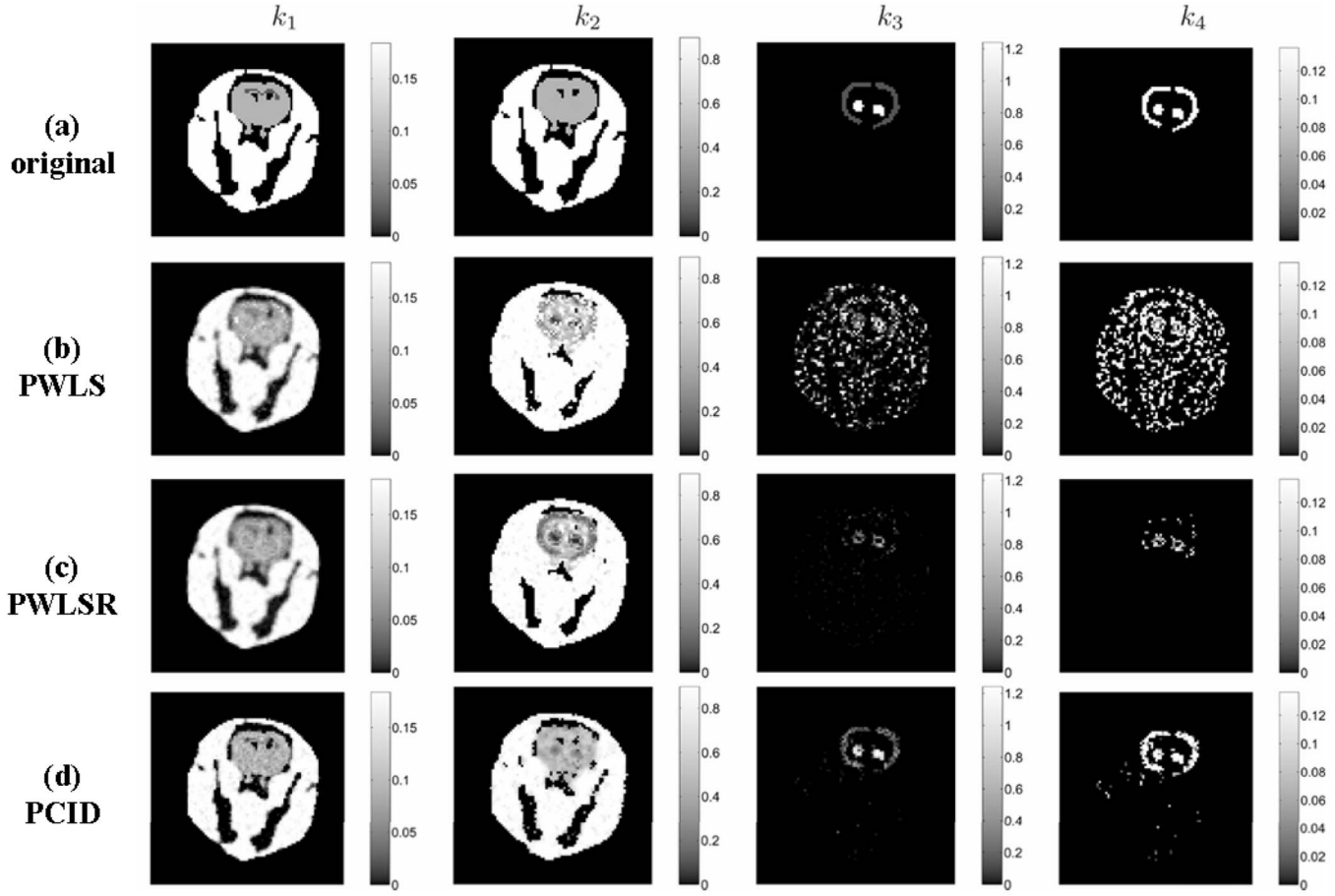

FIG. 7. Parametric images of k_1, k_2, k_3, and k_4 in (a) the original simulation and reconstructed using standard dynamic reconstruction followed by (b) pixelwise weighted least-squares (PWLS) fitting, (c) PWLS with spatial regularization, and finally (d) the proposed direct PICD algorithm. Adapted and reprinted with permission from Ref. 39.

only be applicable when there is a one-to-one correspondence between the anatomical region and the functional region.

VI.B.2. Voxel-based techniques

Kinetic parameter estimation at the voxel level (i.e., generation of parametric images) was achieved directly from dynamic PET data by Kamasak *et al.*[39] The method was implemented for a specific compartmental model: The reversible two-tissue compartmental model with four kinetic parameters (k_1,k_2,k_3,k_4), resulting in a direct parametric iterative coordinate descent (PICD) algorithm. Comparison of results obtained using this method with standard techniques is shown in Fig. 7 for a simulated study and exhibited clear improvements, as also quantitatively demonstrated to result in low root-mean-squared errors for all the four kinetic parameters. In an application of this technique to real data, a method for the evaluation of the exactness of the fit and estimation of error in the kinetic parameters was investigated.[107]

Furthermore, in a work by Yan *et al.*,[46] applied to the simpler one-tissue model, a novel EM algorithm directly estimating each of k_1 and k_2 was proposed. The approach has the advantage of being closed form (and not requiring gradient-search like optimization, as above) and being applicable directly to list-mode data.

The majority of direct parametric reconstruction methods in the past have utilized nonlinear kinetic models to estimate individual kinetic parameters. In contrast to such nonlinear models, a number of graphical modeling methods have been developed that yield simple linear/visual techniques for estimation/evaluation of kinetic properties of various PET tracers and more robust parametric estimates (e.g., see Ref. 103 for a review). The Patlak linear model for irreversible tracer binding was recently included in a direct parametric estimation task by Wang *et al.*[47] wherein the authors expanded the objective function for the reconstruction task to directly relate the Patlak parameters across the image to the measured data and used a preconditioned conjugate gradient algorithm to find the optimum solution.

Within a similar Patlak estimation task, Tsoumpas *et al.*[48] and Tang *et al.*[49] alternatively extended the system matrix formulation and derived a direct 4D EM parametric reconstruction algorithm, having the advantages of being accurate in formulation and having a closed-form expression. This was effectively achieved by utilizing a different hidden

complete-data formulation within the EM method: Instead of the standard, physically intuitive voxel contributions to each detector bin, the contributions of each of the Patlak elements to each bin were utilized as the complete data.[49] Furthermore, even in the context of reversible tracer binding, wherein a recently published graphical analysis technique exhibits linear properties,[104] Rahmim *et al.*[38] proposed a closed-form direct 4D parametric image estimation technique.

Wang and Qi[50] proposed a more generalized formulation applicable to any model in which the parametric image can be linearly related to the measured data (e.g., B-spline, spectral basis, and Patlak models), resulting in a close-formed EM reconstruction algorithm, with a further extension to allow a nested EM algorithm (with rapid subiterative updates) resulting in further acceleration.

One may note that while multiframe PET reconstruction methods using temporal basis functions are linear inverse problems, the tasks of direct parametric estimation when involving nonlinear kinetic models are nonlinear estimation problems, posing an extra layer of difficulty. In an important work by the same authors[51] allowing direct reconstruction of general (including nonlinear) kinetic models, the method of paraboloidal surrogate functions[108] was utilized (which approximates the Poisson log-likelihood function by local parabolas, thus considerably simplifying the optimization task) to derive a feasible direct estimation technique. The method was shown to effectively reduce into two steps at each iteration, one providing temporary intermediate image estimates, and the other a weighted image-based kinetic parameter optimization tasks. The developed algorithm has the great advantage that it is applicable to nonlinear kinetic models, is fairly straightforward to implement, and that the second part resembles the least-squares optimization task as utilized by a wide variety of standard kinetic modeling tasks, except that the weights are now accurately determined and not chosen on an approximate or *ad hoc* basis. It should be noted that convergence issues with this algorithm remain to be studied.

Note that the methods discussed in Sec. III.A.1 can also be considered as direct estimation tasks since the smooth temporal basis functions were based on underlying biological models, and the extracted coefficients conveyed how much each biological factor contributed to the data. This was also the case for the SVD and PCA methods discussed in Sec. III C 1, which, as argued by the authors, would distinguish the separate biological contributions to the collected data. Nevertheless, since these methods all involved the use of smooth temporal basis functions, they were discussed in Sec. III.

Some limitations with regard to the direct parameter estimation technique are that the overall kinetic model has to be known in advance prior to reconstruction and also to apply well to all areas in the image, as assumed by the parametric image-to-data projection framework. The use of graphical models[103] in which a very fixed compartment model does not have to be assumed, and instead the estimated collective parameters can take on different meanings depending on the model assumed postreconstruction, allows an added flexibility and is a move in this direction.

Additionally, in the context of direct parameter estimation, while it is possible to use reference region techniques to avoid blood sampling, such an approach would ordinarily require an initial reconstruction of the dynamic images to extract the reference region, followed by direct parameter estimation reconstruction. Alternative techniques that estimate the plasma input function itself within the 4D reconstruction method have also been investigated.[39,109,110] The stability of the estimates remains to be demonstrated, especially as increasingly unknown sets of kinetic parameters including the plasma function are estimated with these techniques.

VII. FUTURE OPPORTUNITIES AND CHALLENGES

With the widespread availability of multimodality imaging platforms (PET/CT and PET/MR in the near future), it is expected that in the future, we would be able to navigate numerous dimensions through the human body (e.g., 4D anatomical imaging modality as well as its associated contrast agent dynamics, cardiac and/or respiratory gated functional PET imaging, and enabled simultaneous acquisition using a second PET probe targeting another biological function, e.g., tumor hypoxia in addition to glucose metabolism).[111] Thus, multiparametric molecular imaging will likely be the spotlight of medical practice where early and accurate diagnoses and individualized therapy planning will be made by appropriate imaging probes.

In this context, novel parameter estimation techniques making a more "collective" use of the data, as opposed to independent analyses of different portions of the data, will be of much potential. CT- or MR-assisted PET image reconstruction, in which the high resolution anatomical information is utilized to better address the count-rate and resolution limitations of PET imaging, is one such example. Another example is the collective incorporation of the dynamic PET acquisition data within image reconstruction tasks, giving rise to 4D imaging techniques as reviewed in this work. Within this latter area, many novel techniques have already been proposed, and shown to outperform the conventional independent frame reconstruction. At the same time, thorough comparisons between these techniques are still to be performed, and criteria are to be developed for their use in different protocols. Validation and optimization work in this area, though computationally challenging particularly as there is a need for elaborate Monte Carlo studies of dynamic PET imaging, will still be required. In particular, for various techniques reviewed in this work, there remain important outstanding issues to investigate, as Table I touches upon.

The techniques reviewed in this work can also be used for the extension of 4D PET imaging to 5D and higher dimension PET imaging, by including additional dimensions, for instance, coming from gating (cardiac or respiratory or both[112]). In the present applications, concurrent dynamic and gated imaging is rarely performed since standard indepen-

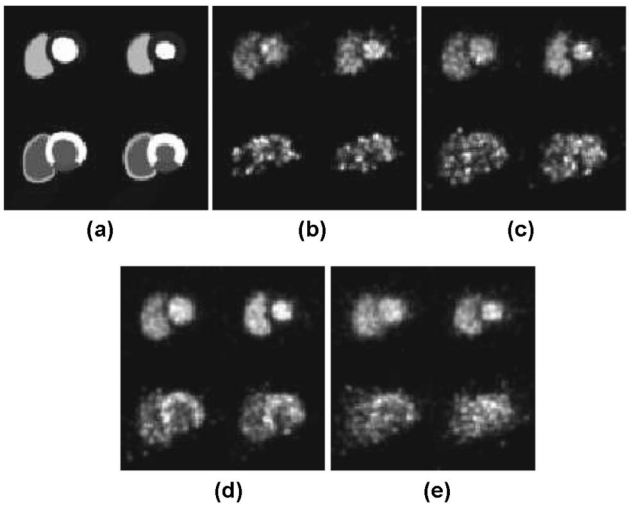

FIG. 8. (a) Short axis view of a simulated cardiac phantom and the resulting images obtained via standard reconstruction (b) without and (c) with postsmoothing, and using (d) first-order and (e) third-order (i.e., cubic) B-spline temporal basis functions in the temporal and gate dimensions. Adapted and reprinted with permission from Ref. 54.

dent reconstruction of the individual dynamic, gated PET data result in considerably noisy images. However, this could be of interest in a number of areas. For instance, in dynamic cardiac imaging, ^{13}N-labeled ammonia ($^{13}NH_3$) can be used for the measurement of myocardial blood flow which makes it possible to measure blood flow at the level of microcirculation. Addition of cardiac gating to dynamic imaging has the advantage of reducing cardiac motion artifacts.

Verhaeghe *et al.*[54] took an interesting step in this direction by using B-spline temporal basis functions (see Sec. III B) to represent both the temporal and gate dimensions. As shown in Fig. 8, standard reconstructions result in noisy images, which upon postsmoothing result in loss of spatial resolution and thus relevant details. By contrast, advanced 5D imaging using temporal basis functions results in improved noise properties while maintaining sharply defined images.

It must however be noted that, as mentioned in Sec. I B 1, dynamic imaging and motion-compensated imaging (e.g., in cardiac) involve different fundamentals. Therefore, even though a number of techniques discussed in this work have also been used in the past for motion-compensated image reconstruction (e.g., temporal smoothing, use of temporal basis functions, PCA), they remain to be validated to provide evidence whether they result in physically allowed estimated motion vectors. Alternatively, they are best treated distinctly and with more direct consideration of motion itself.[52]

There is clear evidence that dynamic PET imaging will find an increasingly important role in various clinical domains including oncology, cardiology, neurology, and psychiatry. Nowadays, a plethora of novel tracers are used routinely for assessing tumor metabolism and other biological and physiological parameters associated with many diseases[113,114] that have clearly demonstrated the enormous potential of PET as an emerging modality in the field of molecular imaging. The application and full exploitation of dynamic imaging taking advantage of 4D reconstruction strategies is well established in research environments and is still limited in clinical settings to institutions with advanced physics and technical support.[20,115–117] As the above mentioned challenges are met, and experience is gained, implementation of validated techniques in commercial software packages will be useful to attract the interest of the clinical community and increase the popularity of this approach. It is expected that with the availability of advanced mathematical models and their algorithmic implementations as well as computing power in the near future, more complex and ambitious algorithms will become clinically feasible. Given that the role of any imaging technique is established with respect to benefits conveyed to patients, what remains to be studied and validated is whether application of 4D image reconstruction techniques to clinical dynamic imaging will result in significant improvements in clinical imaging tasks including clinical diagnosis, assessment of response to treatment, and delivery of personalized treatments and targeted therapies.

Finally, we would like to note that in the works reviewed here, when scatter and random estimations have been performed, they have been done in the context of conventional independent frame reconstruction: i.e., it is always possible to use 4D reconstruction techniques while employing scatter and random corrections as estimated independently for each dynamic frame. Nevertheless, some of the very same motivations for 4D PET image reconstruction are applicable to scatter and random estimations (particularly to scatter estimation as it is typically estimated based on preliminary image estimates): It may be beneficial to incorporate information from data in other frames in this estimation task. In fact, such an approach is further motivated by noting that scatter and random contributions, due to their broad distributions, are less sensitive to variations in image intensities across the frames.[118] It remains to be demonstrated whether such an approach to 4D PET image reconstruction would result in significant improvements in dynamic PET imaging tasks.

VIII. SUMMARY

Molecular imaging using PET is now playing a pivotal role both in a clinical setting and experimental preclinical studies. The important role of multidimensional and multiparametric imaging is growing steadily and gaining acceptance. As diagnostic techniques transition from the systems to the molecular level, the role of multiparametric imaging becomes ever more important.

The present work has attempted to summarize important themes in the emerging field of 4D PET image reconstruction, the objective is to address existing issues with conventional dynamic PET imaging. The issues arising from conventional independent frame reconstruction were outlined, namely, having limited temporal resolution, high noise (especially when higher frame sampling is introduced to capture fast dynamics), as well as the considerable complexity of modeling the generated noise in the images in the kinetic modeling step.

A wide range of techniques designed to address some or all of these issues is discussed, including techniques that utilize (a) iterative temporal smoothing, (b) smooth temporal basis functions, (c) principal components transformation of the dynamic data, (d) wavelet-based techniques, as well as (e) direct kinetic parameter estimation methods. A number of related advantages, drawbacks/limitations, as well as issues to further investigate with each technique were also outlined. Differences between the list-mode and histogram-mode reconstruction techniques were additionally discussed. A number of future opportunities and challenges in the area of 4D and higher dimensional PET image reconstruction were also indicated.

ACKNOWLEDGMENTS

This work was in part supported by the Swiss National Science Foundation under Grant No. SNSF 31003A-125246.

[a]Author to whom correspondence should be addressed. Electronic mail: arahmim1@jhmi.edu; Telephone: +1 410-502-8579; Fax: +1 401-955-0696.

[1]H. Zaidi, *Quantitative Analysis in Nuclear Medicine Imaging* (Springer, New York, 2006).
[2]A. Rahmim, J. C. Cheng, S. Blinder, M. L. Camborde, and V. Sossi, "Statistical dynamic image reconstruction in state-of-the-art high-resolution PET," Phys. Med. Biol. **50**(20), 4887–4912 (2005).
[3]A. Rahmim and H. Zaidi, "PET versus SPECT: Strengths, limitations and challenges," Nucl. Med. Commun. **29**(3), 193–207 (2008).
[4]M. Bentourkia and H. Zaidi, "Tracer kinetic modeling in PET," PET Clin **2**(2), 267–277 (2007).
[5]D. L. Snyder, "Parameter estimation for dynamic studies in emission-tomography systems having list-mode data," IEEE Trans. Nucl. Sci. **31**(2), 925–931 (1984).
[6]H. Barrett, D. Wilson, and B. Tsui, "Noise properties of the EM algorithm: I. Theory," Phys. Med. Biol. **39**(5), 833–846 (1994).
[7]J. Qi, "A unified noise analysis for iterative image estimation," Phys. Med. Biol. **48**, 3505–3519 (2003).
[8]J. Qi and R. M. Leahy, "Iterative reconstruction techniques in emission computed tomography," Phys. Med. Biol. **51**(15), R541–R578 (2006).
[9]A. J. Reader and H. Zaidi, "Advances in PET image reconstruction," PET Clin **2**(2), 173–190 (2007).
[10]C. Tsoumpas, F. E. Turkheimer, and K. Thielemans, "A survey of approaches for direct parametric image reconstruction in emission tomography," Med. Phys. **35**(9), 3963–3971 (2008).
[11]R. J. Walledge, R. Manavaki, M. Honer, and A. J. Reader, "Inter-frame filtering for list-mode EM reconstruction in high-resolution 4-D PET," IEEE Trans. Nucl. Sci. **51**(3), 705–711 (2004).
[12]L. Taek-Soo, W. P. Segars, and B. M. W. Tsui, "Study of parameters characterizing space-time Gibbs priors for 4D MAP-RBI-EM in gated myocardial perfusion SPECT," *IEEE Nuclear Science Symposium Conference Record* (IEEE, New York, 2005), Vol. 4, pp. 2124–2128.
[13]D. J. Kadrmas and G. T. Gullberg, "4D maximum a posteriori reconstruction in dynamic SPECT using a compartmental model-based prior," Phys. Med. Biol. **46**(5), 1553–1574 (2001).
[14]A. J. Reader, J. C. Matthews, F. C. Sureau, C. Comtat, R. Trebossen, and I. Buvat, "Iterative kinetic parameter estimation within fully 4D PET image reconstruction," *IEEE Nuclear Science Symposium Conference Record* (IEEE, New York, 2006), Vol. 3, pp. 1752–1756.
[15]S. R. Meikle, J. C. Matthews, V. J. Cunningham, D. L. Bailey, L. Livieratos, T. Jones, and P. Price, "Parametric image reconstruction using spectral analysis of PET projection data," Phys. Med. Biol. **43**(3), 651–666 (1998).
[16]T. E. Nichols, J. Qi, E. Asma, and R. M. Leahy, "Spatiotemporal reconstruction of list-mode PET data," IEEE Trans. Med. Imaging **21**(4), 396–404 (2002).
[17]Q. Li, E. Asma, S. Ahn, and R. M. Leahy, "A fast fully 4-D incremental gradient reconstruction algorithm for list mode PET data," IEEE Trans. Med. Imaging **26**(1), 58–67 (2007).
[18]J. Verhaeghe, Y. D'Asseler, S. Vandenberghe, S. Staelens, and I. Lemahieu, "An investigation of temporal regularization techniques for dynamic PET reconstructions using temporal splines," Med. Phys. **34**(5), 1766–1778 (2007).
[19]J. Matthews, D. Bailey, P. Price, and V. Cunningham, "The direct calculation of parametric images from dynamic PET data using maximum-likelihood iterative reconstruction," Phys. Med. Biol. **42**(6), 1155–1173 (1997).
[20]A. J. Reader, F. C. Sureau, C. Comtat, R. Trebossen, and I. Buvat, "Joint estimation of dynamic PET images and temporal basis functions using fully 4D ML-EM," Phys. Med. Biol. **51**(21), 5455–5474 (2006).
[21]A. J. Reader, F. Sureau, C. Comtat, R. Trebossen, and I. Buvat, "Simultaneous estimation of temporal basis functions and fully 4D PET images" *IEEE Nuclear Science Symposium Conference Record* (IEEE, New York, 2006), Vol. 4, pp. 2219–2223.
[22]M. N. Wernick, E. J. Infusino, and M. Milosevic, "Fast spatio-temporal image reconstruction for dynamic PET," IEEE Trans. Med. Imaging **18**(3), 185–195 (1999).
[23]M. V. Narayanan, M. A. King, E. J. Soares, C. L. Byrne, P. H. Pretorius, and M. N. Wernick, "Application of the Karhunen-Loeve transform to 4D reconstruction of cardiac gated SPECT images," IEEE Trans. Nucl. Sci. **46**(4), 1001–1008 (1999).
[24]P. Millet, V. Ibanez, J. Delforge, S. Pappata, and J. Guimon, "Wavelet analysis of dynamic PET data: Application to the parametric imaging of benzodiazepine receptor concentration," Neuroimage **11**(5), 458–472 (2000).
[25]J. W. Lin, A. F. Laine, and S. R. Bergmann, "Improving PET-based physiological quantification through methods of wavelet denoising," IEEE Trans. Biomed. Eng. **48**(2), 202–212 (2001).
[26]J. W. Lin, A. F. Laine, O. Akinboboye, and S. R. Bergmann, "Use of wavelet transforms in analysis of time-activity data from cardiac PET," J. Nucl. Med. **42**(2), 194–200 (2001).
[27]F. E. Turkheimer, R. B. Banati, D. Visvikis, J. A. D. Aston, R. N. Gunn, and V. J. Cunningham, "Modeling dynamic PET-SPECT studies in the wavelet domain," J. Cereb. Blood Flow Metab. **20**(5), 879–893 (2000).
[28]F. E. Turkheimer, J. A. D. Aston, R. B. Banati, C. Riddell, and V. J. Cunningham, "A linear wavelet filter for parametric imaging with dynamic PET," IEEE Trans. Med. Imaging **22**(3), 289–301 (2003).
[29]Z. Cselényi, H. Olsson, L. Farde, and B. Gulyás, "Wavelet-aided parametric mapping of cerebral dopamine D2 receptors using the high affinity PET radioligand [11C]FLB 457," Neuroimage **17**(1), 47–60 (2002).
[30]L. Arhjoul and M. H. Bentourkia, "Study of myocardial glucose metabolism in rats with PET using wavelet analysis techniques," Comput. Med. Imaging Graph. **29**(5), 357–365 (2005).
[31]J. Verhaeghe, D. Van De Ville, I. Khalidov, Y. D'Asseler, I. Lemahieu, and M. Unser, "Dynamic PET reconstruction using wavelet regularization with adapted basis functions," IEEE Trans. Med. Imaging **27**(7), 943–959 (2008).
[32]L. Arhjoul and M. Bentourkia, "Assessment of glucose metabolism from the projections using the wavelet technique in small animal PET imaging," Comput. Med. Imaging Graph. **31**(3), 157–165 (2007).
[33]E. Tsui and T. F. Budinger, "Transverse section imaging of mean clearance time," Phys. Med. Biol. **23**(4), 644–653 (1978).
[34]S. C. Huang, R. E. Carson, and M. E. Phelps, "Measurement of local blood flow and distribution volume with short-lived isotopes: A general input technique," J. Cereb. Blood Flow Metab. **2**(1), 99–108 (1982).
[35]N. M. Alpert, L. Eriksson, J. Y. Chang, M. Bergstrom, J. E. Litton, J. A. Correia, C. Bohm, R. H. Ackerman, and J. M. Taveras, "Strategy for the measurement of regional cerebral blood flow using short-lived tracers and emission tomography," J. Cereb. Blood Flow Metab. **4**(1), 28–34 (1984).
[36]R. E. Carson, S. C. Huang, and M. V. Green, "Weighted integration method for local cerebral blood flow measurements with positron emission tomography," J. Cereb. Blood Flow Metab. **6**, 245–258 (1986).
[37]R. P. Maguire, C. Calonder, and K. L. Leenders, in *Quantification of Brain Function Using PET*, edited by V. C. R. Myers, D. Bailey, and T. Jones (Academic, San Diego, 1996), pp. 307–311.
[38]A. Rahmim, Y. Zhou, and J. Tang, "Direct 4D parametric image estimation in reversible tracer binding imaging [abstract]," J. Nucl. Med. **50**(5), 137P–138P (2009).
[39]M. E. Kamasak, C. A. Bouman, E. D. Morris, and K. Sauer, "Direct reconstruction of kinetic parameter images from dynamic PET data," IEEE Trans. Med. Imaging **24**(5), 636–650 (2005).
[40]R. E. Carson and K. Lange, "The EM parametric image reconstruction

algorithm," J. Am. Stat. Assoc. **80**, 20–22 (1985).
[41]E. Vanzi, A. R. Formiconi, D. Bindi, G. LaCava, and A. Pupi, "Kinetic parameter estimation from renal measurements with a three-headed SPECT system: A simulation study," IEEE Trans. Med. Imaging **23**(3), 363–373 (2004).
[42]R. H. Huesman, B. W. Reutter, G. L. Zeng, and G. T. Gullberg, "Kinetic parameter estimation from SPECT cone-beam projection measurements," Phys. Med. Biol. **43**(4), 973–982 (1998).
[43]G. L. Zeng, G. T. Gullberg, and R. H. Huesman, "Using linear time-invariant system theory to estimate kinetic parameters directly from projection measurements," IEEE Trans. Nucl. Sci. **42**(6), 2339–2346 (1995).
[44]P-C Ciao, W. L. Rogers, N. H. Clinthorne, J. A. Fessler, and A. O. Hero, "Model-based estimation for dynamic cardiac studies using ECT," IEEE Trans. Med. Imaging **13**(2), 217–226 (1994).
[45]P-C Ciao, W. L. Rogers, J. A. Fessler, N. H. Clinthorne, and A. O. Hero, "Model-based estimation with boundary side information or boundary regularization [cardiac emission CT]," IEEE Trans. Med. Imaging **13**(2), 227–234 (1994).
[46]J. Yan, B. Planeta-Wilson, and R. E. Carson, "Direct 4D list mode parametric reconstruction for PET with a novel EM algorithm," *IEEE Nuclear Science Symposium Conference Record*, edited by B. Yu (IEEE, New York, 2008), pp. 3625–3628.
[47]G. Wang, L. Fu, and J. Qi, "Maximum a posteriori reconstruction of the Patlak parametric image from sinograms in dynamic PET," Phys. Med. Biol. **53**(3), 593–604 (2008).
[48]C. Tsoumpas, F. E. Turkheimer, and K. Thielemans, "Study of direct and indirect parametric estimation methods of linear models in dynamic positron emission tomography," Med. Phys. **35**(4), 1299–1309 (2008).
[49]J. Tang, H. Kuwabara, D. F. Wong, and A. Rahmim, "Direct 4D reconstruction of parametric images incorporating anato-functional joint entropy," *IEEE Nuclear Science Symposium Conference Record*, edited by B. Yu (IEEE, New York, 2008), pp. 5471–5474.
[50]G. Wang and J. Qi, "Accelerate direct reconstruction of linear parametric images using nested algorithms," *IEEE Nuclear Science Symposium Conference Record*, edited by B. Yu (IEEE, New York, 2008), pp. 5468–5470.
[51]G. Wang and J. Qi, "Iterative nonlinear least squares algorithms for direct reconstruction of parametric images from dynamic PET," *5th IEEE International Symposium on Biomedical Imaging: From Nano to Macro* (IEEE, New York, 2008), pp. 1031–1034.
[52]A. Rahmim, O. G. Rousset, and H. Zaidi, "Strategies for motion tracking and correction in PET," PET Clin **2**, 251–266 (2007).
[53]N. Grotus, A. J. Reader, S. Stute, J. C. Rosenwald, P. Giraud, and I. Buvat, "Fully 4D list-mode reconstruction applied to respiratory-gated PET scans," Phys. Med. Biol. **54**(6), 1705–1721 (2009).
[54]J. Verhaeghe, Y. D'Asseler, S. Staelens, S. Vandenberghe, and I. Lemahieu, "Reconstruction for gated dynamic cardiac PET imaging using a tensor product spline basis," IEEE Trans. Nucl. Sci. **54**(1), 80–91 (2007).
[55]A. J. Reader, K. Erlandsson, M. A. Flower, and R. J. Ott, "Fast accurate iterative reconstruction for low-statistics positron volume imaging," Phys. Med. Biol. **43**(4), 835–846 (1998).
[56]H. H. Barrett, T. White, and L. C. Parra, "List-mode likelihood," J. Opt. Soc. Am. A Opt. Image Sci. Vis. **14**(11), 2914–2923 (1997).
[57]R. H. Huesman, G. J. Klein, W. W. Moses, J. Qi, B. W. Reutter, and P. R. Virador, "List-mode maximum-likelihood reconstruction applied to positron emission mammography (PEM) with irregular sampling," IEEE Trans. Med. Imaging **19**(5), 532–537 (2000).
[58]C. Byrne, "Likelihood maximization for list-mode emission tomographic image reconstruction," IEEE Trans. Med. Imaging **20**(10), 1084–1092 (2001).
[59]A. Rahmim, M. Lenox, A. J. Reader, C. Michel, Z. Burbar, T. J. Ruth, and V. Sossi, "Statistical list-mode image reconstruction for the high resolution research tomograph," Phys. Med. Biol. **49**(18), 4239–4258 (2004).
[60]A. J. Reader, S. Ally, F. Bakatselos, R. Manavaki, R. J. Walledge, A. P. Jeavons, P. J. Julyan, S. Zhao, D. L. Hastings, and J. Zweit, "One-pass list-mode EM algorithm for high-resolution 3-D PET image reconstruction into large arrays," IEEE Trans. Nucl. Sci. **49**(3), 693–699 (2002).
[61]A. Rahmim, P. Bloomfield, S. Houle, M. Lenox, C. Michel, K. R. Buckley, T. J. Ruth, and V. Sossi, "Motion compensation in histogram-mode and list-mode EM reconstructions: beyond the event-driven approach," IEEE Trans. Nucl. Sci. **51**, 2588–2596 (2004).
[62]D. S. Lalush, C. Lin, and B. M. W. Tsui, "A priori motion models for four-dimensional reconstruction in gated cardiac SPECT," *IEEE Nuclear Science Symposium Conference Record*, Anaheim, CA, 2–9 November 1996 (IEEE, New York, 1996), Vol. 3, pp. 1923–1927.
[63]E. J. Gravier and Y. Yang, "Motion-compensated reconstruction of tomographic image sequences," IEEE Trans. Nucl. Sci. **52**(1), 51–56 (2005).
[64]E. Gravier, Y. Yang, M. A. King, and M. Jin, "Fully 4D motion-compensated reconstruction of cardiac SPECT images," Phys. Med. Biol. **51**(18), 4603–4619 (2006).
[65]V. J. Cunningham and T. Jones, "Spectral analysis of dynamic PET studies," J. Cereb. Blood Flow Metab. **13**(1), 15–23 (1993).
[66]K. S. Nijran and D. C. Barber, "Towards automatic analysis of dynamic radionuclide studies using principal-components factor analysis," Phys. Med. Biol. **30**(12), 1315–1325 (1985).
[67]M. Zibulevsky, "ML reconstruction of dynamic PET images from projections and Clist," *IEEE Nuclear Science Symposium Conference Record* (IEEE, New York, 1999), Vol. 2, pp. 889–891.
[68]R. M. Lewitt, "Alternatives to voxels for image representation in iterative reconstruction algorithms," Phys. Med. Biol. **37**(3), 705–716 (1992).
[69]S. Matej and R. M. Lewitt, "Practical considerations for 3-D image reconstruction using spherically symmetric volume elements," IEEE Trans. Med. Imaging **15**(1), 68–78 (1996).
[70]M. H. Byonocore, W. R. Brody, and A. Macovski, "A natural pixel decomposition for two-dimensional image reconstruction," IEEE Trans. Biomed. Eng. **BME-28**(2), 69–78 (1981).
[71]J. R. Baker, T. F. Budinger, and R. H. Huesman, "Generalized approach to inverse problems in tomography: Image reconstruction for spatially variant systems using natural pixels," Crit. Rev. Biomed. Eng. **20**(1–2), 47–71 (1992).
[72]S. Vandenberghe, S. Staelens, C. L. Byrne, E. J. Soares, I. Lemahieu, and S. J. Glick, "Reconstruction of 2D PET data with Monte Carlo generated system matrix for generalized natural pixels," Phys. Med. Biol. **51**(12), 3105–3125 (2006).
[73]M. Unser, "Splines: A perfect fit for signal and image processing," IEEE Signal Process. Mag. **16**, 22–38 (1999).
[74]M. Unser, "Sampling-50 years after Shannon," Proc. IEEE **88**(4), 569–587 (2000).
[75]P. Thevenaz, T. Blu, and M. Unser, "Interpolation revisited (medical images application)," IEEE Trans. Med. Imaging **19**(7), 739–758 (2000).
[76]F. O'Sullivan, "Metabolic images from dynamic positron emission tomography studies," Stat. Methods Med. Res. **3**, 87–101 (1994).
[77]F. O'Sullivan, "Locally constrained mixture representation of dynamic imaging data from PET and MR studies," Biostat **7**(2), 318–338 (2006).
[78]F. O'Sullivan, Y. Pawitan, and D. Haynor, "Reducing negativity artifacts in emission tomography: Post-processing filtered backprojection solutions," IEEE Trans. Med. Imaging **12**(4), 653–663 (1993).
[79]P. Razifar, J. Axelsson, H. Schneider, B. Langstrom, E. Bengtsson, and M. Bergstrom, "Volume-wise application of principal component analysis on masked dynamic PET data in sinogram domain," IEEE Trans. Nucl. Sci. **53**(5), 2759–2768 (2006).
[80]P. Razifar, J. Axelsson, H. Schneider, B. Langstrom, E. Bengtsson, and M. Bergstrom, "A new application of pre-normalized principal component analysis for improvement of image quality and clinical diagnosis in human brain PET studies—clinical brain studies using [11C]-GR205171, [11C]-L-deuterium-deprenyl, [11C]-5-Hydroxy-L-Tryptophan, [11C]-L-DOPA and Pittsburgh Compound-B," Neuroimage **33**(2), 588–598 (2006).
[81]P. Razifar, A. Ringheim, H. Engler, H. Hall, and B. Langstrom, "Masked-volume-wise PCA and "reference Logan" illustrate similar regional differences in kinetic behavior in human brain PET study using [11C]-PIB," BMC Neurol. **9**, 2 (2009).
[82]K. J. Friston, C. D. Frith, P. F. Liddle, and R. S. Frackowiak, "Functional connectivity: the principal-component analysis of large (PET) data sets," J. Cereb. Blood Flow Metab. **13**(1), 5–14 (1993).
[83]F. Pedersen, M. Bergstrom, E. Bengtsson, and B. Langstrom, "Principal component analysis of dynamic positron emission tomography images," Eur. J. Nucl. Med. **21**(12), 1285–1292 (1994).
[84]G. Zuendorf, N. Kerrouche, K. Herholz, and J. C. Baron, "Efficient principal component analysis for multivariate 3D voxel-based mapping of brain functional imaging data sets as applied to FDG-PET and normal aging," Hum. Brain Mapp. **18**(1), 13–21 (2003).
[85]T. Thireou, L. G. Strauss, A. Dimitrakopoulou-Strauss, G. Kontaxakis, S. Pavlopoulos, and A. Santos, "Performance evaluation of principal com-

ponent analysis in dynamic FDG-PET studies of recurrent colorectal cancer," Comput. Med. Imaging Graph. **27**(1), 43–51 (2003).
[86]C.-M. Kao, J. T. Yap, J. Mukherjee, and M. N. Wernick, "Image reconstruction for dynamic PET based on low-order approximation and restoration of the sinogram," IEEE Trans. Med. Imaging **16**(6), 738–749 (1997).
[87]G. El Fakhri, A. Sitek, B. Guerin, M. F. Kijewski, M. F. Di Carli, and S. C. Moore, "Quantitative dynamic cardiac 82Rb PET using generalized factor and compartment analyses," J. Nucl. Med. **46**(8), 1264–1271 (2005).
[88]Y. Su, M. J. Welch, and K. I. Shoghi, "The application of maximum likelihood factor analysis (MLFA) with uniqueness constraints on dynamic cardiac microPET data," Phys. Med. Biol. **52**(8), 2313–2334 (2007).
[89]D. Montgomery, A. Amira, and H. Zaidi, "Fully automated segmentation of oncological PET volumes using a combined multiscale and statistical model," Med. Phys. **34**(2), 722–736 (2007).
[90]D. L. Donoho, I. M. Johnstone, G. Kerkyacharian and D. Picard, "Wavelet shrinkage—asymptopia," J. R. Stat. Soc. Ser. B (Methodol.) **57**(2), 301–337 (1995).
[91]F. Abramovich and B. W. Silverman, "Wavelet decomposition approaches to statistical inverse problems," Biometrika **85**(1), 115–129 (1998).
[92]E. D. Kolaczyk, "A wavelet shrinkage approach to tomographic image reconstruction," J. Am. Stat. Assoc. **91**(435), 1079–1090 (1996).
[93]D. L. Donoho and I. M. Johnstone, "Ideal spatial adaptation by wavelet shrinkage," Biometrika **81**(3), 425–455 (1994).
[94]M. A. T. Figueiredo and R. D. Nowak, "An EM algorithm for wavelet-based image restoration," IEEE Trans. Image Process. **12**(8), 906–916 (2003).
[95]M. Bhatia, W. C. Karl, and A. S. Willsky, "A wavelet-based method for multiscale tomographic reconstruction," IEEE Trans. Med. Imaging **15**(1), 92–101 (1996).
[96]R. D. Nowak and E. D. Kolaczyk, "A statistical multiscale framework for Poisson inverse problems," IEEE Trans. Inf. Theory **46**(5), 1811–1825 (2000).
[97]T. Frese, C. A. Bouman, and K. Sauer, "Adaptive wavelet graph model for Bayesian tomographic reconstruction," IEEE Trans. Image Process. **11**(7), 756–770 (2002).
[98]N. Y. Lee and Y. Choi, "A modified OSEM algorithm for PET reconstruction using wavelet processing," Comput. Methods Programs Biomed. **80**(3), 236–245 (2005).
[99]J. Nuyts and J. A. Fessler, "A penalized-likelihood image reconstruction method for emission tomography, compared to postsmoothed maximum-likelihood with matched spatial resolution," IEEE Trans. Med. Imaging **22**(9), 1042–1052 (2003).
[100]J. W. Stayman and J. A. Fessler, "Compensation for nonuniform resolution using penalized-likelihood reconstruction in space-variant imaging systems," IEEE Trans. Med. Imaging **23**(3), 269–284 (2004).
[101]J. Nuyts, K. Baete, D. Beque, and P. Dupont, "Comparison between MAP and postprocessed ML for image reconstruction in emission tomography when anatomical knowledge is available," IEEE Trans. Med. Imaging **24**(5), 667–675 (2005).
[102]E. Asma, R. Manjeshwar, and K. Thielemans, "Theoretical comparison of motion correction techniques for PET image reconstruction," *IEEE Nuclear Science Symposium Conference Record* (IEEE, New York, 2006), Vol. 3, pp. 1762–1767.
[103]J. Logan, "Graphical analysis of PET data applied to reversible and irreversible tracers," Nucl. Med. Biol. **27**(7), 661–670 (2000).
[104]Y. Zhou, W. Ye, J. R. Brasic, A. H. Crabb, J. Hilton, and D. F. Wong, "A consistent and efficient graphical analysis method to improve the quantification of reversible tracer binding in radioligand receptor dynamic PET studies," Neuroimage **44**(3), 661–670 (2009).
[105]S.-C. Huang and Y. Zhou, "Spatially-coordinated regression for image-wise model fitting to dynamic PET data for generating parametric images," IEEE Trans. Nucl. Sci. **45**(3), 1194–1199 (1998).
[106]Y. Zhou, S.-C. Huang, and M. Bergsneider, "Linear ridge regression with spatial constraint for generation of parametric images in dynamic positron emission tomography studies," IEEE Trans. Nucl. Sci. **48**(1), 125–130 (2001).
[107]E. D. Morris, M. E. Kamasak, B. T. Christian, T. E. Cheng, and C. A. Bouman, "Visualizing all the fits: Evaluating the quality and precision of parametric images created from direct reconstruction of PET sinogram data," *3rd IEEE International Symposium on Biomedical Imaging: Macro to Nano* (IEEE, New York, 2006), pp. 291–294.
[108]J. A. Fessler and H. Erdogan, "A paraboloidal surrogates algorithm for convergent penalized-likelihood emission image reconstruction," *IEEE Nuclear Science Symposium Conference Record* (IEEE, New York, 1998), Vol. 2, pp. 1132–1135.
[109]I. S. Yetik and J. Qi, "Direct estimation of kinetic parameters from the sinogram with an unknown blood function," *Proceedings of the Third IEEE International Symposium on Biomedical Imaging: Nano to Macro*, Arlington, VA, 6–9 April 2006 (IEEE, New York, 2006), pp. 295–298.
[110]A. J. Reader, J. C. Matthews, F. C. Sureau, C. Comtat, R. Trebossen, and I. Buvat, "Fully 4D image reconstruction by estimation of an input function and spectral coefficients," *IEEE Nuclear Science Symposium Conference Record* (IEEE, New York, 2007), Vol. 5, pp. 3260–3267.
[111]H. Zaidi, "Navigating beyond the 6th dimension: A challenge in the era of multi-parametric molecular imaging," Eur. J. Nucl. Med. Mol. Imaging **36**(7), 1025–1028 (2009).
[112]A. Martinez-Möller, D. Zikic, R. Botnar, R. Bundschuh, W. Howe, S. Ziegler, N. Navab, M. Schwaiger, and S. Nekolla, "Dual cardiac respiratory gated PET: Implementation and results from a feasibility study," Eur. J. Nucl. Med. Mol. Imaging **34**(9), 1447–1454 (2007).
[113]G. Antoni and B. Langstrom, "Radiopharmaceuticals: Molecular imaging using positron emission tomography," in *Molecular Imaging I*, edited by W. Semmler and M. Schwaiger (Springer, Berlin, Germany, 2008), Vol. 185, Pt. 1, pp. 177–201.
[114]R. Kumar, H. Dhanpathi, S. Basu, D. Rubello, S. Fanti, and A. Alavi, "Oncologic PET tracers beyond [(18)F]FDG and the novel quantitative approaches in PET imaging," Q. J. Nucl. Med. Mol. Imaging **52**(1), 50–65 (2008).
[115]T. Li, B. Thorndyke, E. Schreibmann, Y. Yang, and L. Xing, "Model-based image reconstruction for four-dimensional PET," Med. Phys. **33**(5), 1288–1298 (2006).
[116]F. Lamare, M. J. Ledesma Carbayo, T. Cresson, G. Kontaxakis, A. Santos, C. Cheze Le Rest, A. J. Reader, and D. Visvikis, "List-mode-based reconstruction for respiratory motion correction in PET using non-rigid body transformations," Phys. Med. Biol. **52**(17), 5187–5204 (2007).
[117]F. Qiao, T. Pan, J. W. Clark, and O. R. Mawlawi, "Region of interest motion compensation for PET image reconstruction," Phys. Med. Biol. **52**(10), 2675–2689 (2007).
[118]J. C. Cheng, A. Rahmim, S. Blinder, M. L. Camborde, K. Raywood, and V. Sossi, "A scatter-corrected list-mode reconstruction and a practical scatter/random approximation technique for dynamic PET imaging," Phys. Med. Biol. **52**(8), 2089–2106 (2007).